Applied Chemistry Today **19(73)** (2024) 257-268

Semnan University

Applied Chemistry Today

Journal homepage: https://chemistry.semnan.ac.ir/

ISSN: 2981-2437

Research Article

Fabrication of a New Polymeric Transdermal Patch Modified by Mesoporous Filler

Mahya Samari[a], Soheila Kashanian[a,b*], Sirus Zinadini[a,c], Hossein Derakhshankhah[d,e]

[a]*Department of Applied Chemistry, Faculty of Chemistry, Razi University, Kermanshah, Iran*

[b]*Nanobiotechnology Department, Faculty of Innovative Science and Technology, Razi University, Kermanshah, Iran*

[c]*Environmental Research Center (ERC), Razi University, Kermanshah, Iran*

[d]*Pharmaceutical Sciences Research Center, Health Institute, Kermanshah University of Medical Sciences, Kermanshah, Iran*

[e]*USERN Office, Kermanshah University of Medical Sciences, Kermanshah, Iran*

PAPER INFO

Article history:
Received: 20/Jul/2024
Revised: 07/Dec/2024
Accepted: 29/Dec/2024

Keywords:
Mesoporous filler,
Polymeric membrane,
Transdermal drug delivery,
Azithromycin.

ABSTRACT

This study developed an advanced drug delivery system featuring an asymmetric PES-based membrane enhanced with modified SBA-15 to enhance the transdermal delivery of azithromycin. The research aimed to optimize membrane performance by adjusting key parameters like drug concentration, membrane thickness, and modifier percentage. Various techniques were used to evaluate the performance of the fabricated membranes, including scanning electron microscopy, water contact angle measurements, hemocompatibility tests, and antibacterial assessments. Following the optimization, a membrane composition of 17% PES, 2% polyvinylpyrrolidone (PVP), and 1% modified SBA-15 was found to be the most effective. The optimized membranes showed significantly enhanced drug release compared to unmodified ones. This improvement was attributed to the membrane's unique structure, which includes a dense top layer for sustained drug release and a porous sub-layer serving as a drug reservoir. Biocompatibility tests, antibacterial activity analysis, and blood compatibility evaluations indicated that the optimized membranes are biocompatible. The findings demonstrated that the modified membranes are effective in enhancing drug delivery and are safe for potential clinical applications.

DOI: https://doi.org/10.22075/chem.2025.34683.2288

* **.corresponding author:** Professor of Clinical Biochemistry. *E-mail address: kashanian_s@yahoo.com*

How to cite this article: Samari, M., Kashanian, S., Zinadini, S. & Derakhshankhah, H. (2024). Fabrication of a New Polymeric Transdermal Patch Modified by Mesoporous Filler. *Applied Chemistry Today*, **19(73)**, 257-268. (in Persian)

1. Introduction

In pharmacotherapy, sustained-release drug delivery systems are frequently essential for effectively managing chronic diseases. These therapeutic strategies involve administering maintenance medications, which are critical for improvement of health outcomes [1-3]. While, the prolonged usage of these medications can introduce several challenges, including poor absorption [4, 5], first-pass metabolism [6, 7], dosage limitations [8, 9], adherence issues [10, 11], storage and stability concerns [12, 13], cost implications [14], and adverse effects [15,38]. These potential risks necessitate careful monitoring and management by healthcare professionals. To overcome these challenges, multiple drug delivery routes have been explored, including oral [16], inhalation [17], intravenous [18], subcutaneous [19], and transdermal methods [20]. Notably, transdermal delivery routes are widely utilized, including transdermal patches [21], transdermal gels and creams [23], iontophoresis [24], and microneedle systems [25].

Transdermal patches (TPs) present an advanced drug delivery system designed to transport medications into the bloodstream [21,39]. This method finds usage across diverse therapeutic domains [26]. TP offers various advantages; improved patient compliance, controlled drug release, lower risk of side effects [27,40]. However, the efficiency of TPs may vary depending on design and the inherent characteristics of the drug.

Polyethersulfone (PES) is a kind of synthetic polymer widely employed in fabrication of the TPs for drug delivery through the skin. Its use is favoured due to excellent properties [28, 29]. In TPs, PES often use as a backing layer, offering mechanical strength and safeguarding the active ingredients enclosed within the patch [30]. PES has gained popularity for its beneficial attributes and its capability to uphold mechanical strength and barrier integrity over prolonged periods.

SBA-15 is a mesoporous silica material known for its ordered hexagonal array of cylindrical mesopores, offering significant potential in materials science and nanotechnology [31,42]. It is synthesized using templating methods, where a surfactant molecule acts as a template around which the silica precursor polymerizes; subsequent removal of the surfactant creates the ordered mesoporous structure. SBA-15 exhibits exceptional properties [32], including customizable pore size and excellent thermal and chemical stability, which contribute to its versatility. These attributes make SBA-15 suitable for a wide range of applications, including drug delivery, sensing, catalysis, and separation processes. Its biocompatibility, adjustable pore size, and controlled drug release kinetics further enhance its appeal as a promising candidate in advanced drug delivery systems [33, 34].

The focus of this study is on developing efficient and safe TPs. This approach leverages a diffusion-based mechanism to release drugs from the pores of the membrane. Critical parameters such as membrane thickness (ranging from 150 to 600 µm), drug concentration (500 to 1500 mg/L), and modifier percentage (0.5% to 2% of modified SBA-15) were optimized to achieve the desired DDS performance.

2. Materials and Methods

2.1. Materials

A range of chemicals was used in this experimental study. Pluronic P123 ($(EO)_{20}(PO)_{70}(EO)_{20}$, was obtained from Sigma-Aldrich Co., USA. Polyethersulfone (PES) was sourced from BASF Co., Germany. Azithromycin (99.9%), imidazole, dimethylacetamide (DMAc), tetraethoxysilane (TEOS, 98%), ethylenediaminetetraacetic acid (EDTA), N,N'-dicyclohexylcarbodiimide (DCC),

dimethylformamide (DMF) and HCl (37%), were acquired from Merck Co., Germany.

2.2. Synthesis of modified SBA-15

For the synthesis of SBA-15 initially, a mixture containing Pluronic P123 (4 g), HCl (125 mL, 2M), and distilled water (50 mL) was prepared. TEOS (10 mL) was then added to the mixture, which was continuously stirred for 24 hours. Following the stirring process, the mixture was heated 100°C for 24 hours. The resulting product was subsequently washed with distilled water, filtered, and dried [35]. To synthesize thio-imidazole@SBA-15 (modified SBA-15), 5 g of EDTA, 0.5 g of imidazole, and 0.2 g of DCC were combined and dissolved in 20 ml of DMF. The solution was then heated under reflux in an oil bath at 100°C for 24 hours. After completion of the reaction, the product was thoroughly rinsed with distilled water and dried in an oven at 60°C for 24 hours. The resulting nanocomposite was subsequently incorporated into the membrane matrix at varying mass fractions.

2.3. Membrane fabrication

Polymeric membranes were prepared using phase inversion techniques [36, 39]. In this investigation, modified SBA-15 served as a membrane modifier to enhance both hydrophilicity and structural properties.

According to Table 1, different amounts of modified SBA-15, PES and PVP, were initially dispersed in DMAc and sonicated. Then, the mixture was stirred continuously for 24 hours to create homogeneous blend with consistent properties.

During membrane fabrication, the solutions were casted onto clean glass plates using a film applicator to achieve specific thicknesses (150-600 µm). The coated plates were then immersed in distilled water, forming flat-sheet polymeric membranes.

After fabrication, the membranes were soaked overnight in fresh distilled water to complete the phase separation process.

Table 1. The formulation of the membrane solutions

Membrane type	PES, wt.%	PVP, wt.%	DMAc wt.%	Modified SBA-15, wt.%
M1	17	2	81	0
M2	17	2	80.5	0.5
M3	17	2	80	1
M4	17	2	79.5	1.5
M5	17	2	79	2

Note: Polyethersulfone (PES), polyvinylpyrrolidone (PVP), dimethylacetamide (DMAc)

2.4. Drug loading

After membrane fabrication the, the drug solution (500-1500 mg/L) was introduced into the membrane texture. A custom Plexiglas setup was used to facilitate this process, ensuring thorough exposure of the membrane sub-layers to the drug solution.

2.5. In vitro drug release

For in vitro drug release investigations [41,43], the drug release was evaluated using Franz diffusion cell.

During the examination, 1 mL of the medium was withdrawn at specified intervals (e.g., 1 h), and an equivalent volume of fresh phosphate buffer saline (PBS) was replenished to maintain sink conditions. The released drug of azithromycin (AZI) in the medium was determined using UV-vis spectrophotometry (208 nm).

2.6. Characterization techniques

The cross-section morphology of the prepared membranes was analysed using a scanning electron microscope (SEM; TESCAN MIRA III).

Fourier transform infrared spectroscopy (FT-IR) was utilized to investigate the chemical bonds present in the membranes. This analysis was conducted using a Bruker alpha spectrometer from Germany.

To evaluate membrane hydrophilicity, water contact angle (WCA) measurements were conducted (contact angle meter XCA-50) [36].

This comprehensive approach facilitates the characterization of membrane morphology, chemical composition, and surface properties crucial for assessing their performance in drug delivery applications. The porosity of the prepared membranes was examined according to the gravimetric method (Equation 1);

$$\varepsilon = \frac{\omega_1 - \omega_2}{A \times L \times dW} \quad (1)$$

Here, ω_2 and ω_1 are the membrane weights before and after submerging into the distilled water. *A*, *L*, and dW are surface diameter (m^2), thickness (m), and water density (999 Kg/m^3), respectively.

2.7. Hemocompatibility Assessment

The hemocompatibility of the fabrications was assessed using real samples. The blood was combined with PBS (1:1.5) and incubated at 37°C for 1 hour. For controls, diluted blood with deionized water was used as a positive control (inducing 100% hemolysis), and PBS served as a negative control (inducing 0% hemolysis).

After the incubation, the samples underwent centrifugation at 1600 rpm for 15 minutes to separate the supernatant. Then the absorbance of the released haemoglobin in the supernatant was measured (545 nm) [37]. This procedure evaluates the membranes' effects on blood components and their compatibility with blood.

2.8. Antibacterial Testing

The antibacterial properties of the prepared membranes were evaluated using the agar disk diffusion method, a standard technique in microbiology. Mueller-Hinton agar was poured into sterile petri dishes and allowed to solidify. A standardized inoculum of each test microorganism (including Gram-positive bacteria such as *Streptococcus sobrinus* and *Staphylococcus aureus*, as well as Gram-negative bacteria like *Pseudomonas aeruginosa* and *Escherichia coli*) was evenly spread across the agar surface.

3. Results

3.1. Characterization of modified SBA-15

The FTIR spectra of SBA-15 reveal distinct peaks that provide valuable insights into its chemical and physical properties. One prominent peak corresponds to the Si-O-Si stretching vibration, typically around 1070 cm^{-1}. This peak indicates the presence of siloxane bonds within the SBA-15 structure, which contribute to its stability and thermal resistance. Another significant peak arises from the Si-OH stretching vibration, commonly found at approximately 950 cm^{-1}. This peak signifies the presence of surface hydroxyl groups on the SBA-15 material. These hydroxyl groups are crucial in various applications, including catalysis and adsorption processes [1-4].

For the M1 membrane, the observed peaks at 1242 cm^{-1} and 1153 cm^{-1} correspond to sulfonic groups ($–SO_3H$). The peak at 1153 cm^{-1} overlaps with the stretching vibrations of ether groups (C–O–C–). Peaks associated with aromatic groups (C=C in the benzene ring) are observed at 1485 cm^{-1} and 1579 cm^{-1}.The peaks observed at 860 cm^{-1} and 840 cm^{-1} correspond to the benzene ring with para-substitution. For the M3 membrane, the observed peaks at 1014 cm^{-1} and 962 cm^{-1} correspond to Si–O stretching vibrations. The remaining peaks overlap with the C–O stretching vibrations (Fig.1).

3.2. SEM images

SEM images were utilized to analyse the structural characteristics and size distribution of modified SBA-15, M1 and M3 membrane (Fig. 2). These images reveal distinctive features that highlight the quality of modified SBA-15 synthesis, showcasing uniformity in size and shape. The modified SBA-15 particles, synthesized following the method described, typically exhibit a nanoscale size range of 80-200 nm, as reported in the literature [37].

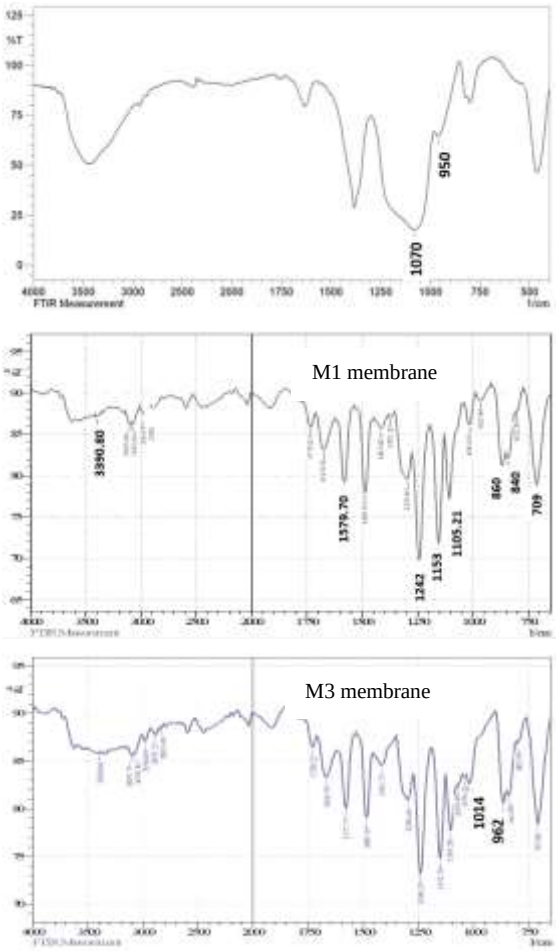

Fig. 1. FTIR spectrum of the bare (M1) and optimal modified membrane (M3)

This uniformity underscores the precise and controlled formation of the mesoporous structure within SBA-15, which is crucial for its applications in various fields such as catalysis, drug delivery, and adsorption processes [5]. The cross-sectional structure of the bare (M1) and optimal modified membrane (M3) was analysed using SEM to gain detailed insights into the effects of the modification on their morphological properties. The analysis revealed that the membranes consisted of a dense, compact top layer (act as controlling layer), which provides selectivity, supported by a porous, finger-like sublayer (act as drug reservoir) that facilitates mechanical stability and permeability. This hierarchical structure is indicative of the phase inversion process used during fabrication, highlighting the successful integration of the modification into the membrane architecture.

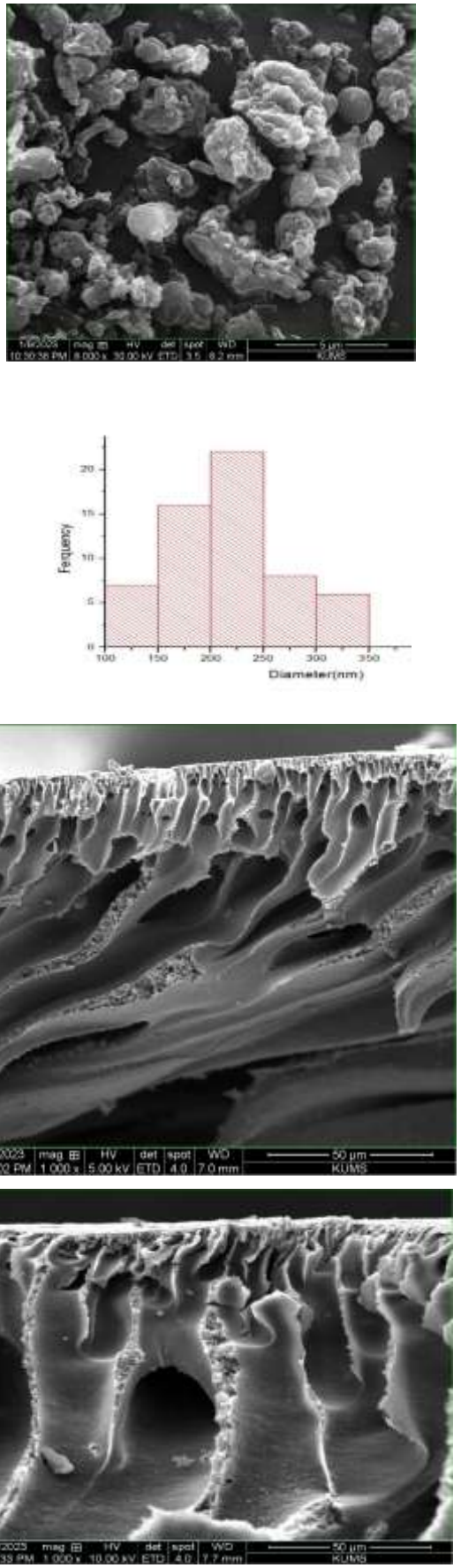

Fig. 2. SEM image of the modified SBA-15 nanoparticle, SBA size distribution, and cross-sectional image of M1 and M3 membrane

3.3. Porosity and Hydrophilicity

The water contact angle (WCA) serves as a key indicator of surface hydrophilicity, with lower WCAs indicating greater affinity for water. In comparison, higher WCAs suggest hydrophobic tendencies, where water droplets bead up due to low surface energy, resisting wetting.

Flat-sheet membranes based on bare PES typically exhibit hydrophobic characteristics characterized by a high WCA [45]. However, the loading of hydrophilic modified SBA-15 into the membrane texture through modification processes can alter these surface properties. This modification leads to a reduction in WCA, signifying enhanced hydrophilicity.

According to the specific case discussed, the WCA decreased for the M3 sample (Fig. 3). This reduction shows that the membrane becomes less hydrophobic following the incorporation of modified SBA-15. Such adjustments are beneficial in applications requiring improved water interaction or enhanced biocompatibility.

This modification of surface properties through modified SBA-15 incorporation enhances the versatility and performance of PES-based membranes in biomedical, filtration, and other technological applications.

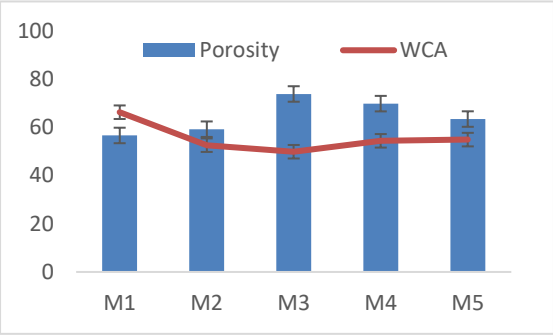

Fig. 3. The water contact angle (WCA) and porosity of the fabricated membranes (n=5)

3.4. Drug release

Fig. 4 illustrates the release profile of AZI (500 mg/L) from the fabricated membranes, providing valuable insights into their release behavior. The data indicate that the optimal performance in AZI release was achieved with membranes modified with 1wt.% SBA-15, reaching a release level of 302.5 mg/L. This optimal release behavior can be attributed to the effect of appropriate filler loading, which facilitated the formation of larger pores within the membrane structure.

Creating these enlarged pores during the polymer film fabrication significantly enhanced the membrane's modification efficiency. Consequently, this modification resulted in the maximum storage capacity for the drug solution, enabling more effective and sustained drug release.

In contrast, the unmodified membrane (M1) exhibited a burst release of AZI within the initial hours, followed by a decline in performance over 24 hours. This behavior can be attributed to the absence of optimized filler and, consequently, the lack of large pores necessary for efficient drug loading and sustained release.

The other modified membranes displayed smaller cavities, primarily due to suboptimal loading amounts of the mesoporous fillers. This reduction in cavity size negatively impacted their drug absorption and release capacity, highlighting the importance of achieving the optimal filler concentration for effective drug delivery.

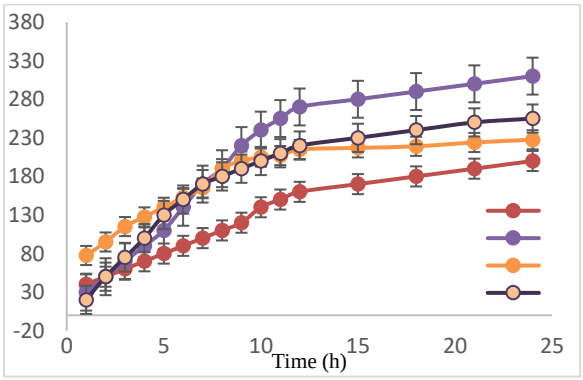

Fig. 4. In vitro drug release profiles of 500 mg/L AZI loaded in the M1– M5 in different filler loading (0.5, 1, 1.5, and 2%) with the Franz diffusion cell in the phosphate buffer saline solution medium pH 7.4

These findings are crucial for selecting appropriately modified membranes, particularly

those loaded with 1 wt. % modified SBA-15, for applications where controlled and sustained drug release is essential. The results demonstrate that optimizing the filler loading is crucial to enhancing the structural and functional properties of the membranes, thereby improving their performance in drug delivery systems.

Based on the drug release profiles obtained from previous experiments, it has been determined that the M3 membrane demonstrates the most effective drug release performance among both unmodified and modified membranes. Increasing the drug loading in the fabricated membranes increases drug release. Fig. 5 illustrates the drug release profiles for different initial drug loadings (500, 1000, and 1500 mg/L). Notably, the drug release rate exhibited an increasing trend with higher initial drug concentrations of 1000 and 1500 mg/L over 24 hours. Various factors, including the physical and chemical properties of the membranes, influence the amount of drug released.

For the M3 membrane, the most favorable drug release profile was observed at an initial drug concentration of 1000 mg/L. This concentration displayed a higher rate of drug absorption and release from the membrane, resulting in a lower retention percentage than the other two concentrations (500 and 1500 mg/L). This optimal performance can be attributed to the balance between adequate drug loading and the membrane's structural properties, facilitating efficient drug release while minimizing initial burst release.

These findings highlight the importance of optimizing initial drug concentration and membrane properties to achieve controlled and sustained drug release, critical for various biomedical applications. The variation in drug release profiles between high and low drug concentrations can be attributed to the hydrophilicity of the membranes, which facilitates the formation of hydrogen bonds between the membrane matrix and the drug solution. This interaction can lead to incomplete drug release at higher concentrations. Conversely, the lower drug concentration (1000 mg/L) exhibits higher water content, leading to the formation of a molecular hydration layer on the surface and within the pores of the membrane. This hydration layer is a protective barrier, preventing excessive drug accumulation and facilitating efficient drug transfer. This aspect of the study provides critical insights into the drug release behavior of modified membranes, underscoring the importance of optimizing both membrane hydrophilicity and drug concentration to achieve optimal drug release efficiency. By considering these parameters, it is possible to enhance the release kinetics and improve the overall performance of DDSs based on modified membranes.

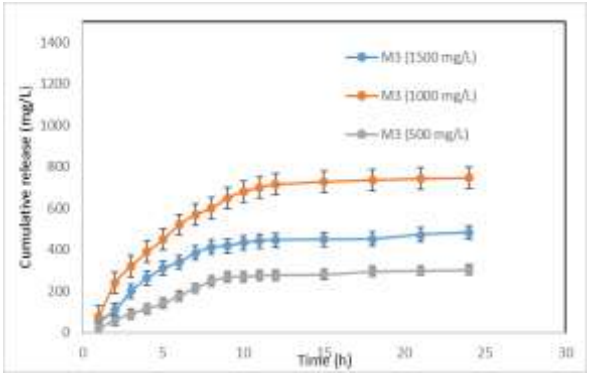

Fig. 5. In vitro, drug release profiles in different drug concentrations loaded in the M3 (as the optimally modified membrane) in the Franz diffusion cell in the phosphate buffer saline solution medium pH 7.4

The thickness of the membrane is a critical factor influencing drug release profiles. Drug release was examined using the optimally modified membrane (M3) at a concentration of 1000 mg/L across different membrane thicknesses (150, 300, 450, and 600 µm) to investigate this. As illustrated in Fig.6, the results revealed that membranes with a thickness of 450 µm exhibited optimal performance in drug release for the M3 membrane. This particular thickness demonstrated the best balance between drug-holding capacity and efficient drug release,

making it the optimal thickness for the fabricated membranes in this study.

Initially, thicker membranes were anticipated to have a greater drug-holding capacity, leading to improved release profiles. However, the study found that increasing membrane thickness decreased drug release. This phenomenon can be attributed to the kinetic and thermodynamic changes during the phase inversion process, particularly for membranes with a thickness of 600 µm. The increased thickness of the casting solution influenced these changes, resulting in smaller membrane pores and reduced drug release.

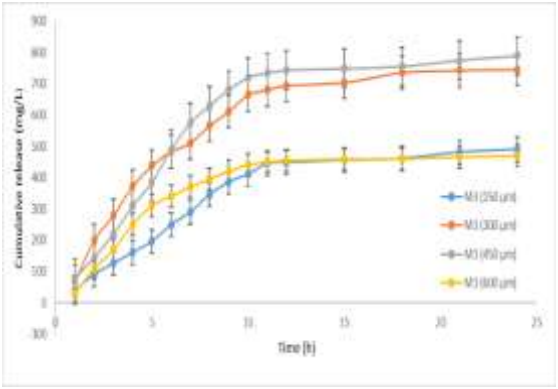

Fig. 6. *In vitro* drug release profiles of the optimally modified membranes (M3) in different membrane thicknesses (150, 300, 450, and 600µm)

3.5. Antibacterial assay

The results of the antibacterial assay indicated that fabricated membranes illustrated superior antibacterial activity (Table 2). This enhancement is attributed to the optimized drug release profile. The presence of the drug embedded in the membranes significantly contributes to their ability to effectively inhibit bacterial growth, demonstrating promising antibacterial activity.

The obtained findings indicated the critical role of optimizing drug release profiles. By ensuring controlled and appropriate drug release, TPs can maintain therapeutic concentrations of the active substance at the application site, thereby enhancing their overall antibacterial performance. This research highlights the potential of modified membranes in advancing the development of more effective antibacterial TPs for clinical and therapeutic applications.

3.6. Hemo-compatibility

Given that the fabricated membranes are intended for application at wound sites, ensuring their compatibility with blood is paramount.

Table 2. The diameter of the inhibition zone of the fabricated membranes

Pathogens	Inhibition zone (mm)		
	M3 + Drug	M1 + Drug	Control
S. sobrinus	16.6±2.0b	12.2±0.0d	13.5±0.1^{c}
P.aeruginosa	32.4±0.6b	22.3±1.5d	29±0.2^{c}
S. aureus	18.0±1.0a	12.0±0.1c	15.4±0.5^{b}
E. coli	16.7±1.5b	11.6±0.1d	14.3±0.7^{c}

Notes: Values are mean ± standard error of triplicates. a-d Means in the same row with different lowercase letters differed significantly ($p < 0.05$)

PES-based transdermal patches are renowned for their hemocompatibility, generally without triggering immune responses. The degree of hemolysis was quantitatively assessed to evaluate the hemo-compatibility of both the M1 and the M3 membrane (M3=4.36%) (Figure 7). The obtained results indicated that the prepared membranes exhibited lower levels of hemolysis compared to the positive control.

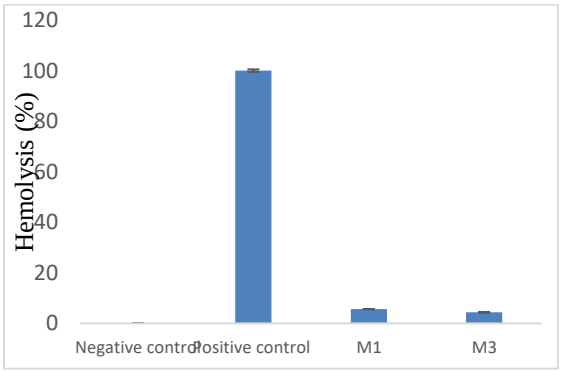

Fig.7. The blood compatibility of the optimally modified (M3) the bare (M1) membranes

4. Conclusion

This study represents a significant advancement in the development of a novel DDS using an asymmetric PES membrane integrated with modified SBA-15. The primary objective was to

optimize membrane performance by refining key parameters.

Through the optimization process, an optimal membrane composition of 17% PES, 2% PVP, and 1% modified SBA-15 was identified. This composition led to a notable enhancement in drug release compared to the bare membrane, owing to its distinctive structural characteristics.

Furthermore, biocompatibility assessments yielded promising outcomes, demonstrating minimal hemolysis of blood cells by the optimized membranes. These findings highlight the potential of the optimized membranes for safe and effective utilization in clinical applications, presenting a promising avenue for advancing drug delivery systems.

Acknowledgment

The authors gratefully acknowledge the financial support of this study by the Razi University.

Conflicts of Interest

The author declares that there is no conflict of interest regarding the publication of this manuscript.

References

[1] Teschke, R., Sarris, J., & Schweitzer, I. (2012). Kava hepatotoxicity in traditional and modern use: the presumed Pacific kava paradox hypothesis revisited. *British journal of clinical pharmacology*, *73*(2), 170-174.

[2] Rombey, T., Puljak, L., Allers, K., Ruano, J., & Pieper, D. (2020). Inconsistent views among systematic review authors toward publishing protocols as peer-reviewed articles: an international survey. *Journal of clinical epidemiology*, *123*, 9-17.

[3] Cheng, H. Y., Jian, S. W., Liu, D. P., Ng, T. C., Huang, W. T., & Lin, H. H. (2020). Contact tracing assessment of COVID-19 transmission dynamics in Taiwan and risk at different exposure periods before and after symptom onset. *JAMA internal medicine*, *180*(9), 1156-1163.

[4] Cutler, W., Kolter, J., Chambliss, C., O'Neill, H., & Montesinos-Yufa, H. M. (2020). Long term absence of invasive breast cancer diagnosis in 2,402,672 pre and postmenopausal women: A systematic review and meta-analysis. Plos one, 15(9), e0237925.

[5] IM, S. (2000). Association of glycemia with macrovascular and microvascular complications of type 2 diabetes (UKPDS 35): prospective observational study. BMJ, 321, 405012.

[6] Chan, K. H., Yan, M., Bennett, D. A., Guo, Y., Chen, Y., Yang, L., ... & China Kadoorie Biobank Study group. (2021). Long-term solid fuel use and risks of major eye diseases in China: A population-based cohort study of 486,532 adults. *PLoS medicine*, *18*(7), e1003716.

[7] Gilhofer, T. S., & Saw, J. (2019). Spontaneous coronary artery dissection: update 2019. *Current Opinion in Cardiology*, *34*(6), 594-602.

[8] Jeong, H. M., Weon, K. Y., Shin, B. S., & Shin, S. (2020). 3D-printed gastroretentive sustained release drug delivery system by applying design of experiment approach. Molecules, 25(10), 2330.

[9] Aithal, G. P., Watkins, P. B., Andrade, R. J., Larrey, D., Molokhia, M., Takikawa, H., ... & Daly, A. K. (2011). Case definition and phenotype standardization in drug-induced liver injury. *Clinical Pharmacology & Therapeutics*, *89*(6), 806-815.

[10] Peppi, M., Marie, A., Belline, C., & Borenstein, J. T. (2018). Intracochlear drug

delivery systems: a novel approach whose time has come. *Expert Opinion on Drug Delivery*, *15*(4), 319-324.

[11] Israel, D. A., Salama, N., Arnold, C. N., Moss, S. F., Ando, T., Wirth, H. P. & Peek, R. M. (2001). Helicobacter pylori strain-specific differences in genetic content, identified by microarray, influence host inflammatory responses. *The Journal of clinical investigation*, *107*(5), 611-620.

[12] Svensson, C. K. (1987). Clinical pharmacokinetics of nicotine. *Clinical pharmacokinetics*, *12*, 30-40.

[13] Stillhart, C., Vučićević, K., Augustijns, P., Basit, A. W., Batchelor, H., Flanagan, T. R. & Müllertz, A. (2020). Impact of gastrointestinal physiology on drug absorption in special populations—An UNGAP review. *European Journal of Pharmaceutical Sciences*, *147*, 105280.

[14] Prandota, J. (1982). Urinary elimination kinetics and diuretic effect of intravenous furosemide in nephrotic children. *Developmental Pharmacology and Therapeutics*, *5*(1-2), 98-108.

[15] Sánchez-Zapardiel, E., Mancebo, E., Díaz-Ordoñez, M., de Jorge-Huerta, L., Ruiz-Martínez, L., Serrano, A. & Paz-Artal, E. (2016). Isolated de novo antiendothelial cell antibodies and kidney transplant rejection. *American Journal of Kidney Diseases*, *68*(6), 933-943.

[16] JE, V. R., Sharpe, L. A., & Peppas, N. A. (2018). Corrigendum to'Current state and challenges in developing oral vaccines'[Adv. Drug Deliv. Rev. 114 (2017) 116-131]. *Advanced Drug Delivery Reviews*, *139*, 158-158.

[17] Petersen, C. (2018). Christine Petersen: Pioneering Leishmania Research in Man and Man's Best Friend. *TRENDS IN PARASITOLOGY*, *34*(7), 543-544.

[18] DiMatteo, M. R., Giordani, P. J., Lepper, H. S., & Croghan, T. W. (2002). Patient adherence and medical treatment outcomes: a meta-analysis. *Medical care*, *40*(9), 794-811.

[19] Osterberg, L., & Blaschke, T. (2005). Adherence to medication. *New England journal of medicine*, *353*(5), 487-497.

[20] Chen, J., Wang, J., Lu, Y., Zhao, S., Yu, Q., Wang, X. & Jiang, Y. (2018). Uncovering potential anti-neuroinflammatory components of Modified Wuziyanzong Prescription through a target-directed molecular docking fingerprint strategy. *Journal of Pharmaceutical and Biomedical Analysis*, *156*, 328-339.

[21] Ruby, P. K., Pathak, S. M., & Aggarwal, D. (2014). Critical attributes of transdermal drug delivery system (TDDS)–a generic product development review. *Drug development and industrial pharmacy*, *40*(11), 1421-1428.

[22] Neumann, P. J. (2021). Toward better data dashboards for US drug value assessments. *Value in Health*, *24*(10), 1484-1489.

[23] Gondo, G. C., Koons, S., Metcalf, C., Bell, S. J., & Mehta, N. N. (2021). Viewing psoriasis as a systemic disease for better health outcomes. *JID Innovations*, *1*(2).

[24] Liu, X., Liu, D., Pan, Y., & Li, Y. (2020). Pharmacokinetic/pharmacodynamics variability of echinocandins in critically ill

patients: A systematic review and meta-analysis. *Journal of Clinical Pharmacy and Therapeutics*, *45*(6), 1207-1217.

[25] Munoz, F., Alici, G., & Li, W. (2014). A review of drug delivery systems for capsule endoscopy. *Advanced drug delivery reviews*, *71*, 77-85.

[26] Shimizu, T., Awata, M., Lila, A. S. A., Yoshioka, C., Kawaguchi, Y., Ando, H., ... & Ishida, T. (2021). Complement activation induced by PEG enhances humoral immune responses against antigens encapsulated in PEG-modified liposomes. *Journal of Controlled Release*, *329*, 1046-1053.

[27] Pena, S. A., Iyengar, R., Eshraghi, R. S., Bencie, N., Mittal, J., Aljohani, A. & Eshraghi, A. A. (2020). Gene therapy for neurological disorders: challenges and recent advancements. *Journal of drug targeting*, *28*(2), 111-128.

[28] Kitayama, K., Maeda, S., Nakamura, A., Katayama, I., & Wataya-Kaneda, M. (2019). Efficiency of sirolimus delivery to the skin is dependent on administration route and formulation. *Journal of Dermatological Science*, *94*(3), 350-353.

[29] Pastore, M. N., Kalia, Y. N., Horstmann, M., & Roberts, M. S. (2015). Transdermal patches: history, development and pharmacology. *British journal of pharmacology*, *172*(9), 2179-2209.

[30] Wong, W. F., Ang, K. P., Sethi, G., & Looi, C. Y. (2023). Recent advancement of medical patch for transdermal drug delivery. *Medicina*, *59*(4), 778.

[31] Bargh, J. D., Isidro-Llobet, A., Parker, J. S., & Spring, D. R. (2019). Cleavable linkers in antibody–drug conjugates. *Chemical Society Reviews*, *48*(16), 4361-4374.

[32] Langer, R. (2004). Transdermal drug delivery: past progress, current status, and future prospects. *Adv. Drug. Deliv. Rev.*, *56*, 557-558.

[33] Xu, T. (2005). Ion exchange membranes: State of their development and perspective. *Journal of membrane science*, *263*(1-2), 1-29.

[34] Qin, Y., Zhu, F., Luo, M., & Zhang, L. (2011). Catalyst-free preparation of polyhedral oligomeric silsesquioxanes containing Organic–Inorganic hybrid mesoporous nanocomposites. *Journal of Applied Polymer Science*, *121*(1), 97-101.

[35] Erkan, D. (2021). Expert perspective: management of microvascular and catastrophic antiphospholipid syndrome. *Arthritis & Rheumatology*, *73*(10), 1780-1790.

[36] Trivedi, J. H. (2013). Synthesis, characterization, and swelling behavior of superabsorbent hydrogel from sodium salt of partially carboxymethylated tamarind kernel powder-g-PAN. *Journal of applied polymer science*, *129*(4), 1992-2003.

[37] Johansson, E. M., Ballem, M. A., Córdoba, J. M., & Odén, M. (2011). Rapid synthesis of SBA-15 rods with variable lengths, widths, and tunable large pores. Langmuir, 27(8), 4994-4999.

[38] Hassani, H., Rezanejad, G., & Kharazmi, H. A. (2024). Synthesis and characterization of porous co-polymeric hydrogels of 2-Hydroxyethyl methacrylate and N-vinyl pyrrolidone via high internal phase

emulsion. *Applied Chemistry Today*, *19*(73), 111-122.

[39] Eshaghi Malekshah, R., Salehi, M., & Khaleghian, A. (2016). Synthesis, characterization and comparative study of cytotoxic effect of copper (II) and zinc β-diketonate complexes. *Applied Chemistry Today*, *11*(41), 165-170.

[40] Nasiri, M., & Abdi, S. (2024). Fabrication and Performance Evaluation of the Polyamide Thin Film Composite Membrane in Desalination and Removal of Naproxen from Aqueous Solutions. *Applied Chemistry Today*, *19*(72), 339-364.

[41] Rezanejad, G., Pargolghasemi, P., & Banaei, A. (2023). Preparation of new macroporous hydrogel by formation of high internal phase emulsions (HIPEs) template and investigation of controlled release of doxorubicin drug. *Applied Chemistry Today*, *18*(68), 251-270.

[42] Khanmohammadi, F., Razavi Zadeh, B. M., & Azizi, S. N. (2023). Nanoparticles of SBA-15 synthesized from corn silica as an effective delivery system for valproic acid. *Applied Chemistry Today*, *17*(65), 65-80.

[43] Azizi, M., Seyed Dorraji, M. S., & Rasoulifard, M. (2018). Preparation of polyurethane nanofibers containing cefixime trihydrate: in vitro release kinetic studies. *Applied Chemistry Today*, *13*(46), 239-248.